

Original Research Article

Open Access



S-nitrosoglutathione reductase (GSNOR) deficiency accelerates cardiomyocyte differentiation of induced pluripotent stem cells

Alessandro G. Salerno, Amarylis C. B. A. Wanschel, Raul A. Dulce, Konstantinos E. Hatzistergos, Wayne Balkan, Joshua M. Hare

Department of Medicine and Interdisciplinary Stem Cell Institute, University of Miami Miller School of Medicine, Miami, FL 33136, USA.

Correspondence to: Dr. Joshua M. Hare, Department of Medicine and Interdisciplinary Stem Cell Institute, University of Miami Miller, Biomedical Research Building, 1501 N. W. 10th Ave, Miami, FL 33136, USA. E-mail: jhare@med.miami.edu

How to cite this article: Salerno AG, Wanschel ACBA, Dulce RA, Hatzistergos KE, Balkan W, Hare JM. S-nitrosoglutathione reductase (GSNOR) deficiency accelerates cardiomyocyte differentiation of induced pluripotent stem cells. *J Cardiovasc Aging* 2021;1:13. <https://dx.doi.org/10.20517/jca.2021.19>

Received: 20 Aug 2021 **First decision:** 31 Aug 2021 **Revised:** 4 Sep 2021 **Accepted:** 4 Sep 2021 **First online:** 7 Sep 2021

Academic Editor: AJ Marian **Copy Editor:** Yue-Yue Zhang **Production Editor:** Yue-Yue Zhang

Abstract

Introduction: Induced pluripotent stem cells (iPSCs) provide a model of cardiomyocyte (CM) maturation. Nitric oxide signaling promotes CM differentiation and maturation, although the mechanisms remain controversial.

Aim: The study tested the hypothesis that in the absence of S-nitrosoglutathione reductase (GSNOR), a denitrosylase regulating protein S-nitrosylation, the resultant increased S-nitrosylation accelerates the differentiation and maturation of iPSC-derived cardiomyocytes (CMs).

Methods and Results: iPSCs derived from mice lacking GSNOR (iPSC^{GSNOR^{-/-}}) matured faster than wildtype iPSCs (iPSC^{WT}) and demonstrated transient increases in expression of murine Snail Family Transcriptional Repressor 1 gene (*Snail*), murine Snail Family Transcriptional Repressor 2 gene (*Slug*) and murine Twist Family BHLH Transcription Factor 1 gene (*Twist*), transcription factors that promote epithelial-to-mesenchymal transition (EMT) and that are regulated by Glycogen Synthase Kinase 3 Beta (GSK3 β). Murine Glycogen Synthase Kinase 3 Beta (*Gsk3 β*) gene exhibited much greater S-nitrosylation, but lower expression in iPSC^{GSNOR^{-/-}}. S-nitrosoglutathione (GSNO)-treated iPSC^{WT} and human (h)iPSCs also demonstrated reduced expression of GSK3 β . *Nkx2.5* expression, a CM marker, was increased in iPSC^{GSNOR^{-/-}} upon directed differentiation toward CMs on Day 4, whereas murine Brachyury (*t*), *Isl1*, and GATA Binding Protein (*Gata4*) mRNA were decreased, compared to iPSC^{WT}, suggesting that



© The Author(s) 2021. **Open Access** This article is licensed under a Creative Commons Attribution 4.0 International License (<https://creativecommons.org/licenses/by/4.0/>), which permits unrestricted use, sharing, adaptation, distribution and reproduction in any medium or format, for any purpose, even commercially, as long as you give appropriate credit to the original author(s) and the source, provide a link to the Creative Commons license, and indicate if changes were made.



GSNOR deficiency promotes CM differentiation beginning immediately following cell adherence to the culture dish-transitioning from mesoderm to cardiac progenitor.

Conclusion: Together these findings suggest that increased S-nitrosylation of Gsk3 β promotes CM differentiation and maturation from iPSCs. Manipulating the post-translational modification of GSK3 β may provide an important translational target and offers new insight into understanding of CM differentiation from pluripotent stem cells.

One sentence summary: Deficiency of GSNOR or addition of GSNO accelerates early differentiation and maturation of iPSC-cardiomyocytes.

Keywords: GSNOR, GSK3 β , differentiation, EMT, cardiomyocytes, iPSCs

INTRODUCTION

The maturation of cardiomyocytes (CM) derived from induced pluripotent (iPS) cells is a highly complex yet incompletely understood process. Endogenous and exogenous nitric oxide (NO) affects stem cell biology and promotes CM maturation, although the mechanism(s) remains controversial^[1,2]. S-nitrosylation (S-NO) of cysteine thiols is a major signaling pathway through which NO exerts its broad regulatory actions^[3,4]. Levels of S-NO in mice are physiologically regulated via the activity of S-nitrosoglutathione (GSNO) reductase [GSNOR (alcohol dehydrogenase 5)], an enzyme that promotes protein denitrosylation. Mice lacking GSNOR (GSNOR^{-/-} mice) show increased levels of S-NO proteins^[5-7]. GSNOR^{-/-} mice have enhanced cardiomyocyte proliferation and recover better than wildtype mice post-myocardial infarction^[8,9]. Here, we hypothesized that the absence of GSNOR, and the resultant increased S-nitrosylation, accelerates the differentiation and maturation of cardiomyocytes. We analyzed early cardiomyogenic differentiation of iPS cells derived from GSNOR^{-/-} and wildtype [WT (control)] mice to test this hypothesis.

Colony structural integrity is crucial for maintaining pluripotency during the expansion of induced pluripotent stem cells (iPSCs) and requires that cells do not undergo epithelial-to-mesenchymal transition (EMT). EMT is a highly ordered process that generates pools of primitive stem/progenitor cells at precise locations within the embryo^[10]. EMT is initiated by the downregulation of intercellular adhesion proteins, such as E-cadherin, the prototypical epithelial adhesion protein, and by the upregulation of EMT-inducing transcription factors, such as Snail (encoded by *SNAI1* and *SNAI2*)^[11]. Glycogen Synthase Kinase 3 Beta (GSK3 β), a serine/threonine kinase, plays a central role in controlling Snail Family Transcriptional Repressor 1 (*Snail*) expression and the Wnt/ β -catenin pathway, an important initiator of EMT^[12]. Modulation of the GSK and Wnt pathways (with small-molecule inhibitors) affects the CM maturation of iPSCs^[13,14]. S-NO of GSK3 β reduces its activity^[15], and inhibition of GSK3 β activity promotes cardiac differentiation and proliferation in murine and human PSCs^[16].

Here, for the first time, we show that GSNOR loss of function promotes EMT, S-NO of GSK3 β , and CM proliferation and differentiation and accelerates the maturation of iPSC-CMs. These findings provide new insights into the modulation of iPSC-cardiomyogenesis and potential cardiac repair targets and cell-based therapy.

MATERIAL AND METHODS

This study was reviewed and approved by the University of Miami Institutional Animal Care and Use Committee (Protocol #20-168) and complies with all federal and state guidelines concerning animals in research and teaching as defined by “The Guide for the Care and Use of Laboratory Animals”^[17].

Animals

The generation of GSNOR^{-/-} mice and their backcrossing for > 10 generations into a C57Bl6/J mouse background (WT) to eliminate/minimize genetic heterogeneity has been reported^[8]. Age-matched WT (C57Bl6/J) mice obtained from Jackson Laboratories were used as controls. Mice received food and water ad libitum and were on a 12-h light/dark cycle. At the endpoint, mice were euthanized by either cervical dislocation or isoflurane inhalation, followed by exsanguination.

Generation of iPSCs

Murine iPSCs derived from GSNOR^{-/-} mice (iPSC^{GSNOR^{-/-}}) and iPSCs derived from the wild type mice (iPSC^{WT}) were generated from fibroblasts isolated from adult heart of 3.5-mo-old male GSNOR^{-/-} and WT mice, respectively, using a commercially available kit (STEMCCA, Millipore). Briefly, hearts were minced and fibroblasts at passage one plated on gelatin-coated 12-well plates at a density of 2×10^4 cells per well (Day 0) with Dulbecco's modified eagle media (DMEM) (Gibco), 2 mM l-glutamine, 10% (vol/vol) fetal bovine serum (FBS) (ES-Gibco), and 1% penicillin-streptomycin (Gibco). The next day (Day 1), cells were transduced with lentiviral particles (STEMCCA cassette). The STEMCCA cassette is a humanized excisable system containing all four reprogramming factors POU Class 5 Homeobox 1, SRY-Box Transcription Factor 2 (SOX2) Kruppel Like Factor 4, and *c-MYC* in a single "stem cell cassette" (pHAGE2-EF1aFull-hOct4-F2A-hKlf4-IRES-hSox2-P2A-hcMyc-W-loxP). The reprogramming Kit was used at a multiplicity of infection (MOI) of 100, followed by a repeated infection at an MOI of 75 on Day 2. Approximately 48 h later, cells were collected by trypsinization and replated onto fresh plates coated with irradiated mouse embryonic fibroblasts (MEFs; Millipore) and fed with mouse ES medium [DMEM, 2 mM l-glutamine, 20% (vol/vol) FBS (ES-Gibco), 0.1 mM nonessential amino acids (Gibco), 0.1 mM 2-mercaptoethanol (Gibco), and 1,000 units/mL Leukemia inhibitory factor (LIF) (Millipore)] supplemented with a cocktail of small molecules to enhance reprogramming (Mouse iPS reprogramming Boost Supplement, Millipore). iPSC colonies began to emerge on Day 7. Each colony was manually picked and individually transferred to fresh plates coated with MEFs. A total of 12 iPSC^{GSNOR^{-/-}} and 10 iPSC^{WT} clones were generated. Clones 9 and 11 for iPSC^{GSNOR^{-/-}} and clones 6 and 10 for iPSC^{WT} were selected and expanded for this study. No variability was observed between studied clones. All iPSC lines were grown on MEFs and adapted gradually to a modified ES + 2i medium [DMEM, l-glutamine, 20% (vol/vol) knockout serum replacement (Gibco), 0.1 mM nonessential amino acids, 0.1 mM 2-mercaptoethanol, 1000 units/mL LIF, 1 μ M PD0325901 (Tocris) and 3 μ M CHIR99021 (Tocris)]. The human induced pluripotent stem cell (hiPSC) line SC101A (System Biosciences) was maintained in E8 medium (ThermoFisher Scientific) under feeder-free conditions on Matrigel-coated plates (BD Biosciences). Cardiac differentiation of human pluripotent stem cells (hPSCs) was performed according to the previously described protocol for directed differentiation via small molecule modulation^[18].

GSNOR activity in whole heart lysates and iPSCs

The GSNOR activity assay was performed as previously described^[8]. Briefly, heart tissues from WT and GSNOR^{-/-} male mice were minced/homogenized in a cell lysis buffer (Cell Signaling). The protein concentration of these samples was determined using a standard Bradford assay. Heart homogenate (200 μ g/mL) were incubated with Tris-HCl (2 mmol/L, pH 8.0), Ethylenediaminetetraacetic acid (EDTA) (0.5 mmol/L), and nicotinamide adenine dinucleotide (NADH) (200 μ mol/L). The reaction was started by adding S-nitrosoglutathione (GSNO) (400 μ mol/L), and activity was measured as GSNO-dependent NADH consumption at an absorbance of 340 nm for 10 min.

Gene-expression analysis

Total RNA was extracted from iPSC^{GSNOR^{-/-}}, iPSC^{WT} and human induced pluripotent stem cells (hiPSCs) at selected time points before and during their differentiation into cardiomyocytes, using the RNeasy mini

plus kit, according to the manufacturers' instructions (Qiagen). cDNA synthesis was performed using the high-capacity cDNA reverse-transcription kit, according to the manufacturer's instructions (Applied Biosystems). Quantitative PCR was performed using Taqman Universal Master mix in an iQ5 real-time PCR (qRT-PCR) detection system (Bio Rad). All samples were run in triplicates and normalized to a GAPDH/18s endogenous control. Relative fold-change was calculated using the $\Delta\Delta C_t$ method. In addition, Taqman Gene-expression assays were performed for the following murine genes: *t*, alcohol Dehydrogenase 5 (Class III) (*Adh5*), *Snail1*, *Snail2*, *E-cadherin*, POU Class 5 Homeobox gene (*Oct4*), *Sox2*, Kruppel Like Factor 4, murine gene (*Klf4*), Glycogen Synthase Kinase 3 Beta gene (*Gsk3 β*), ATPase Sarcoplasmic/Endoplasmic Reticulum Ca²⁺ Transporter 2, murine gene (*Atp2a2*), Ryanodine Receptor 2 (*RyR2*), *Tnni1*, *Tnni3*, *Tnnt2*, *Myh6*, *Myh7*, *Axin1*, *Axin2*, *Twist*, Mesoderm Posterior BHLH Transcription Factor 1 gene (*Mesp1*), *Isl1*, *Nkx2.5*, GATA Binding Protein 4 gene (*Gata4*). (See [Supplementary Table 1](#) for full details of primer/probe sequences).

MTT assay

MTT assays were carried out on Day 4 to 5 of the differentiation process. Cell viability was measured by using Vybrant® MTT Cell Proliferation Assay Kit (Invitrogen by ThermoFisher Scientific) according to the manufacturer's protocol (Quick Protocol Option). Cells were plated in 24-well plates at the density of 2.5×10^4 cells/well. Briefly, the cells were labeled with MTT and incubated for 4 h at 37 °C. Then, DMSO was added to each well and incubated at 37 °C for 10 min to dissolve the formazan. Absorbance at a wavelength of 540 nm was measured in a Spectromax M5 spectrophotometer (Spectra Max; Molecular Devices, Sunnyvale, CA, USA) using software: SoftMaxPro 6.5.1.

Bromodeoxyuridine proliferation assay

Bromodeoxyuridine (BrdU) is incorporated into the newly synthesized DNA strands of actively proliferating cells. According to the manufacturer's protocol, we determined cell proliferation using a BrdU Cell Proliferation enzyme-linked immunosorbent assay kit (Abcam, ab126556, USA). Briefly, 10, 20, or 30 embryoid bodies (EBs) were seeded in a 96-well plate and received BrdU (20 μ L). After 3 (Day 5) or 24 (Day 4-5) h of incubation (37 °C, 5% CO₂), cells were fixed, permeabilized and the DNA denatured. Next, Anti-BrdU monoclonal antibodies were added and incubated for 1 hour. Absorbance was then obtained using a Spectromax M5 spectrophotometer (Spectra Max; Molecular Devices, Sunnyvale, CA, USA) at a wavelength of 450 nm.

Beating cells

Video files were captured using a Zeiss Axio Vert.A1 inverted microscope under phase contrast. The resulting video file was then processed into digitized representations of moving pixels, after which the sum of moving pixels was plotted vs. time. Finally, 10-s segments of these videos were employed for the visual plots.

Migration assay

Cell migration was detected using the Transwell system (Corning, Inc., Corning, NY, USA). Cells (1.5×10^5) were trypsinized and seeded into the upper chamber. After incubation for 24 h at 37 °C, the cells that had migrated into the lower compartment were fixed with methanol, stained with a 5% crystal violet solution, and counted. Each experiment was conducted with at least four replicates, and migrated cells were counted in a minimum of 3 microscope fields.

Western blotting

For Western blotting, cell lysates were prepared by re-suspending iPSC-derived embryoid bodies in RIPA lysis buffer (R0278, Sigma) and protease inhibitor (Complete protease inhibitor cocktail; Roche Molecular

Biochemicals). Proteins (25-40 µg/lane) were electrophoresed through 8%-10% polyacrylamide-SDS gel and then transferred to the nitrocellulose membrane. Membranes were immunostained overnight at 4 °C with primary Axin 1 (1:1000, Cell Signaling Technology, #2087), Gsnor (1:1000, Proteintech, 11051-1-AP), Hsp90 (1:1000, Cell Signaling Technology, #4874), T-brachyury (1:1000, Abcam, ab20680) antibodies and 1 h at room temperature with secondary anti-rabbit IgG (1:2000, Cell Signaling Technology, #7074) and anti-goat IgG (1:2000, Santa Cruz, sc-2384) antibodies. The signal was visualized using the SuperSignal™ West Femto Maximum Sensitivity Substrate (Thermo Scientific™, #34094).

Resin-assisted capture of S-nitrosothiols (SNO-RAC) assay

S-nitrosothiols (SNO)-RAC assays were performed in the dark as described^[19]. Briefly, iPSCs were homogenized in HEN buffer (250 mM HEPES, 1 mM EDTA, and 0.1 mM neocuproine, pH 7.7). Free cysteine residues were blocked with MMTS and reacted with or without sodium ascorbate. Protein lysate was incubated with thiol-reactive resin (Sigma-Aldrich) for 5 h. Resin-captured proteins were eluted using 50 µL elution buffer (20 mM HEPES, 100 mM NaCl, 1 mM EDTA, 100 mM β-mercaptoethanol) and heated at 95 °C for 5 min in reducing SDS-PAGE loading buffer. The expression of murine Glycogen Synthase Kinase 3 Beta protein (Gsk3β) was determined by Western blot analysis.

Cytosolic calcium measurement

Intracellular Ca²⁺ was measured using the Ca²⁺-sensitive dye Fura-2 and a dual-excitation spectrofluorometer (IonOptix LLC, Milton, MA, USA). Briefly, cells were loaded with 2.5 µM Fura-2 for 20 min at room temperature in Tyrode's buffer containing (in mM): 144 NaCl, 1 MgCl₂, 10 HEPES, 5.6 glucose, 5 KCl, 1.2 NaH₂PO₄, 1.5 CaCl₂ (adjusted to a pH 7.4 with NaOH). Then the cells were washed with fresh regular Tyrode's solution for at least 10 min. Cells were excited with a xenon lamp at 340 nm and 380 nm wavelengths. The emission fluorescence (510 ± 15 nm) was collected by a photomultiplier and subsequently integrated by the system's interface. The Ca²⁺ signal was recorded under spontaneous cardiomyocyte contractile activity or electric field-paced (20 V) at different frequencies from 0.5 to 4 Hz. The calibration was performed in cardiomyocytes by superfusing a free Ca²⁺ and then a Ca²⁺ saturating (5 mmol/L) solutions, both containing 10 µmol/L ionomycin (Sigma, St. Louis, MO) until reaching a minimal (R_{min}) or a maximal (R_{max}) ratio value, respectively. (Ca²⁺)_i was calculated as previously in Dulce *et al.*^[3] using the following equation:

$$[Ca^{2+}]_i = K_d \times \frac{S_{f2}}{S_{b2}} \times \frac{(R - R_{min})}{(R_{max} - R)}$$

K_d (dissociation constant) in adult myocytes was taken as 224 nmol/L. The scaling factors S_{f2} and S_{b2} were extracted from calibration^[3].

Calcium transient kinetics and sarcoplasmic reticulum function

We measured the time to reach the (Ca²⁺) transient peak and the time of decaying from the peak to 50% over baseline (tt50%). We also assessed the time constant (τ) of Ca²⁺ decay from a regular twitch and after a pulse of 20 mM caffeine to block the sarcoplasmic reticulum (SR) re-uptake both in regular conditions (1.5 mM CaCl₂) and in the absence of Na⁺ and Ca²⁺ to block the Na⁺/Ca²⁺ exchanger (NCX) activity as well. Using these parameters, we calculated the proportional contribution of sarco(endo)plasmic reticulum Ca²⁺-ATPase, human protein (SERCA), NCX, and other non-NCX mechanisms in mouse induced pluripotent stem cells (miPSCs)-derived CMs by comparing the time constants of Ca²⁺ decay in the following conditions:

- Regular twitch $1/\tau_{\text{twitch}} = K_{\text{SERCA}} + K_{\text{NCX}} + K_{\text{non-NCX}}$
- Caffeine challenge (1.5 mM CaCl₂) $1/\tau_{\text{Caff}} = K_{\text{NCX}} + K_{\text{non-NCX}}$
- Caffeine challenge (0Na⁺/0Ca²⁺) $1/\tau_{\text{Caff0Na/0Ca}} = K_{\text{non-NCX}}$

where K represent the time constant for each depicted mechanism.

Statistics

Statistical analyses were performed using GraphPad Prism version 9.00 for Mac. Values were analyzed using Student's *t*-test or two-way ANOVA. All data met the assumptions of the tests. Therefore, a *P* < 0.05 was considered statistically significant. All values are reported as mean ± SEM (*n* is noted in the figures).

RESULTS

S-nitrosylation status is linked to early cardiomyogenesis in murine iPSCs

Nitric oxide synthase inhibitors prevent the maturation of mESCs into differentiated cardiomyocytes, a process that can be readily rescued by NO donors^[20]. To investigate the effect of NO-mediated protein S-nitrosylation during early cardiomyogenesis in our miPSC model, we used an NADH-dependent GSNOR activity assay to gauge GSNOR enzymatic activity in GSNOR^{-/-} and C57Bl6/J wild type (WT) minced adult heart. As expected, in the presence of GSNO, NADH oxidation produced a sharp decrease in absorbance in WT but not in GSNOR^{-/-} lysates over time [Figure 1A]. Murine iPSC^{GSNOR^{-/-}} and iPSC^{WT} from these adult heart-minced fibroblasts were generated after virus infection using the OSKM factors protocol^[21]. Spontaneous differentiation of iPSCs into beating cardiomyocytes subsequent to the formation of 3-dimensional EBs was seen, as depicted in the schematic experimental approach [Figure 1B]. EBs were grown in hanging drops for the first two days and neither *Gsnor* gene expression nor protein levels were observed in the iPSC^{GSNOR^{-/-}} cells on Day 0 to Day 6 of the differentiation process [Figure 1C and D]. In addition, to provide some characterization on the pluripotency of our cells, we observed an accelerated loss of pluripotency markers such as *Oct4*, *Sox2* and *Klf4* in both groups, but, in the iPSC^{GSNOR^{-/-}} group on Day 6, *Oct4* and *Sox2* were significantly lower than control iPSCs. In contrast, *Klf4* expression, which is also involved in proliferation and differentiation^[22], was higher in iPSC^{GSNOR^{-/-}} on Day 2 but not at later timepoints [Figure 1E].

Finally, the morphology of EB differentiation was examined over a period of 6 days (Day 0-6). The formation and maintenance of the EB population remained relatively uniform until Day 4, at which point, we observed continuous proliferation/differentiation and apparent EMT only in the iPSC^{GSNOR^{-/-}}. Thus, we demonstrated that the genetic deletion of GSNOR is directly associated with differences at the early stages of miPSC growth.

GSNOR deletion stimulates cell proliferation and migration in murine iPSCs

NO, as described above, can influence the proliferation and differentiation cascades of certain cell types^[23,24]. Indeed, S-nitrosylation may be integral to NO function during a variety of cellular processes. We previously described that GSNOR^{-/-} mice exhibit the enhanced proliferative activity of adult cardiac progenitors and cardiomyocytes post-myocardial infarction^[9]. Therefore, we next examined the effect of GSNOR deletion on cell proliferation and migration in miPSCs. An MTT assay was performed on Day 5 and showed that iPSC^{GSNOR^{-/-}} have a higher proliferative (metabolic) activity compared to iPSC^{WT} (0.096 ± 0.006 vs. 0.12 ± 0.006; *P* < 0.05) [Figure 2A]. We observed enhanced BrdU incorporation in iPSC^{GSNOR^{-/-}} EBs (20 and 30 EBs/well) compared with WT [Figure 2B and C], in agreement with the results of the MTT assay, which also

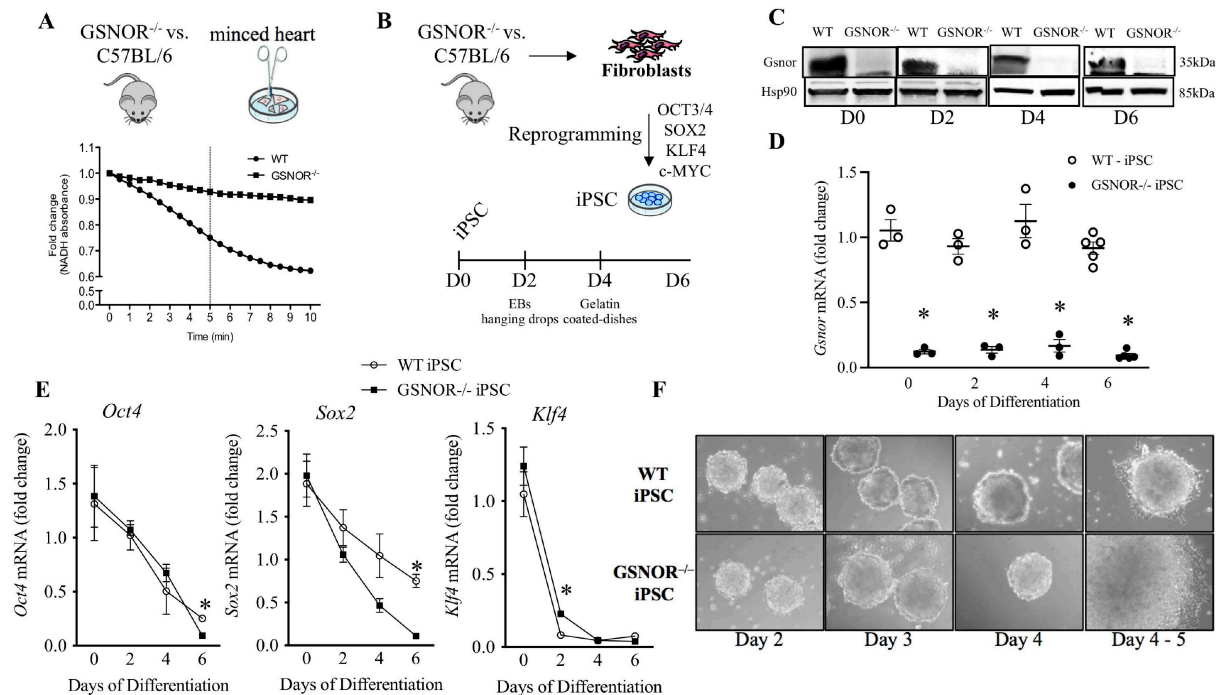


Figure 1. GSNOR loss of function accelerates cardiomyocyte differentiation of murine iPSCs. (A) GSNOR activity in whole heart lysates of GSNOR^{-/-} and C57BL/6 mice. (B) Schematic representation of cardiomyocyte differentiation procedure from Day 0 to Day 6. (C) Western blot analysis of *Gsnor* and Hsp90 (internal control) in murine iPSC^{WT} and iPSC^{GSNOR^{-/-}} during cardiomyocyte differentiation. (D) qRT-PCR analysis of *Gsnor* in murine iPSC^{WT} and iPSC^{GSNOR^{-/-}} during cardiomyocyte differentiation. (E) qRT-PCR analysis of pluripotent genes (*Oct4*, *Sox2*, *Klf4*) in murine iPSC^{WT} (open circles) and iPSC^{GSNOR^{-/-}} (black boxes) during cardiomyocyte differentiation. (F) Morphology of embryoid bodies from iPSC^{WT} (top) and iPSC^{GSNOR^{-/-}} (bottom) over a time course of 5 days. Data are the mean \pm SEM of 3 independent experiments. *P*-values were calculated using Student's *t*-test. **P* < 0.05.

indicated increased proliferation. We also investigated if the absence of GSNOR activity promotes cell migration in addition to proliferation. To quantify migration, cells were seeded into the upper chamber of a transwell dish and after 24 h of incubation; cells that migrated were counted and stained with crystal violet solution. We observed that cellular migration increased by 75% in iPSC^{GSNOR^{-/-}} compared with iPSC^{WT} [Figure 2D], 3.3 ± 0.16 vs. 5.8 ± 0.3 ; *P* < 0.05). Representative micrographs at Day 4 are shown in Figure 2E. These results demonstrate that iPSC^{GSNOR^{-/-}} exhibit increased cellular migration and proliferation compared to iPSC^{WT}.

GSNOR deletion reduces Gsk3 β and increase Axin 1 and Axin 2 in iPSC^{GSNOR^{-/-}}

As mentioned above, S-nitrosylation of GSK3 β inhibits its kinase activity independent of the canonical phospho-inhibition pathway^[15]. Furthermore, inhibition of GSK3 is sufficient to induce CM cell cycle re-entry, DNA synthesis, and likely proliferation^[16]. We hypothesized that GSNOR loss of function increases GSK3 β S-nitrosylation and decreases *Gsk3 β* expression/functionality during the initial growth and differentiation of iPSCs. To test this hypothesis, we first measured mRNA levels of *Gsk3 β* from Day 0 to Day 6. iPSC^{GSNOR^{-/-}} showed significantly reduced expression levels of *Gsk3 β* on Day 4 compared to iPSC^{WT} [Figure 3A]. We next performed SNO-RAC assays^[19] on iPSC^{WT} and iPSC^{GSNOR^{-/-}}. S-nitrosylated proteins were captured by thiol-reactive resin, and Gsk3 β S-nitrosylation status was assessed by immunoblotting. iPSC^{GSNOR^{-/-}} demonstrated greater S-nitrosylation of Gsk3 β compared to iPSC^{WT} [Figure 3B]. The identification of endogenous S-NO in the SNO-RAC assay was validated by the omission of ascorbate, which prevents S-nitrosothiols (SNOs) from being reduced. Furthermore, we examined if increased NO levels in iPSC^{WT}, mimic the effects of the suppressed *Gsk3 β* levels seen in iPSC^{GSNOR^{-/-}}. For these experiments,

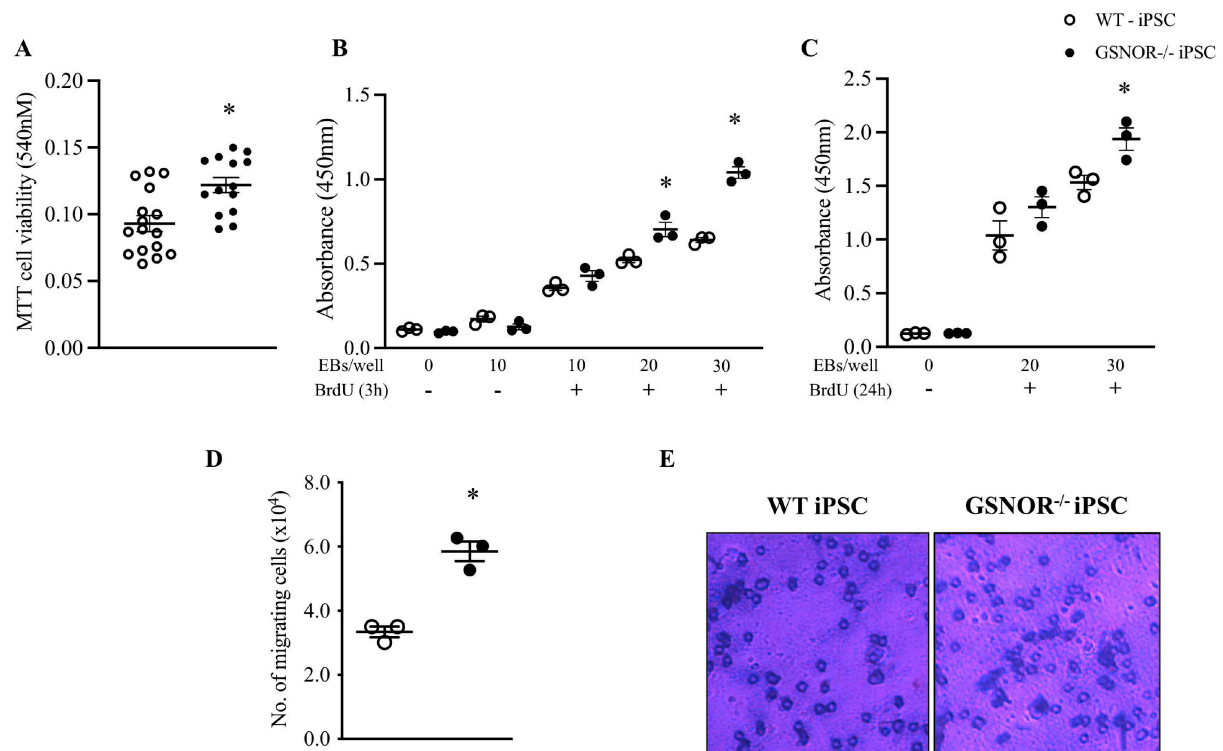


Figure 2. GSNOR loss of function stimulates cell proliferation and cell migration in murine iPSCs. (A) Cell viability as measured by MTT assay on Day 4 in murine iPSC^{GSNOR^{-/-}} and iPSC^{WT}. EBs (4000-5000 cells/EB) from murine iPSC^{WT} (white circles) and iPSC^{GSNOR^{-/-}} (black circles) were incubated with BrdU and proliferation determined following short- (3 h, B), and long-term (24 h, C) plating of different numbers of EBs (4000-5000 cells/EB). (D) Average number of murine iPSC^{GSNOR^{-/-}} and iPSC^{WT} that migrated over a 24-h period. E, Micrograph of cells that migrated and then stained with crystal violet. Data are the mean \pm SEM of 3 independent experiments. *P*-values were calculated using Student's *t*-test at each time point. **P* < 0.05.

we examined three different concentrations of the NO donor, GSNO, 25 μ M, 125 μ M and 250 μ M for 3 h on Day 4 of differentiation. We observed that GSNO decreased *Gsk3 β* expression in iPSC^{WT} cells by 40% [Figure 3C]. The same experiment was performed in hiPSC using two different concentrations of GSNO (100 μ M and 250 μ M) for 24 h on Day 2 of cell culture, a time point that appears to be equivalent to murine iPSC on Day 4^[25]; human Glycogen Synthase Kinase 3 Beta gene (*GSK3 β*) expression was reduced by ~50% with 100 μ M GSNO (*P* < 0.05) compared to control [Figure 3D]. These studies demonstrated that increased S-nitrosylation or exposure to a pharmacologic NO donor reduces GSK3 β expression in iPSCs.

Axin, a scaffold protein, that forms a complex with GSK3 β and β -catenin and promotes GSK3 β -dependent phosphorylation of β -catenin, thereby stimulating the degradation of β -catenin. *Axin 1* and *Axin 2* share a number of structural and functional properties, including homologous GSK3 β -binding domains. Surprisingly, *Axin 1* protein and mRNA expression on Day 4 [Figure 3D and E], and *Axin 2* mRNA expression, on Day 2 were increased in iPSC^{GSNOR^{-/-}} compared to iPSC^{WT} [Figure 3F]. These results suggest that aberrant S-NO/NO levels impact multiple components of the β -catenin regulatory pathway.

EMT-related transcription factors *twist*, *slug*, and *snail* are upregulated, and *E-cadherin* is downregulated in murine iPSC^{GSNOR^{-/-}} and in hiPSCs treated with GSNO

Previously described, inhibition of GSK3 β stimulates the transcription of Snail, a repressor of E-cadherin and inducer of EMT^[26]. Similar cooperative activities suggest that Twist and Snail work synergistically to induce EMT^[27]. Since migration, proliferation and EMT are closely related processes, we tested whether

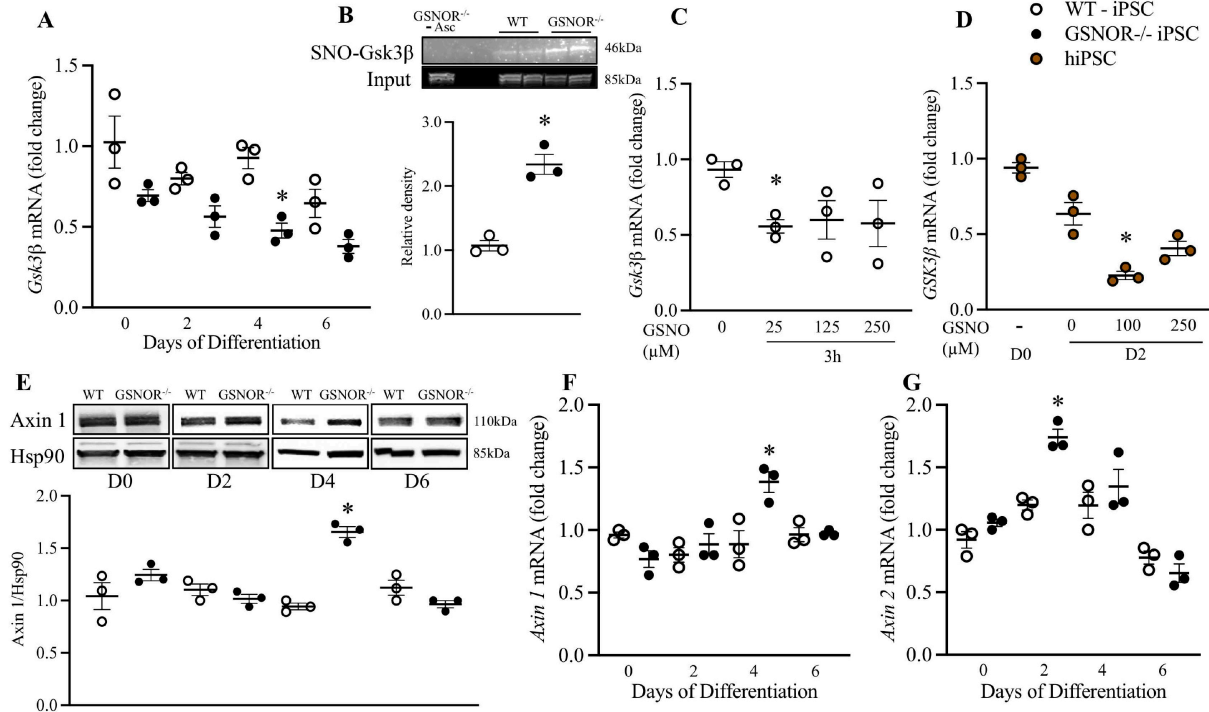


Figure 3. GSNOR loss of function alters S-nitrosylation and expression of *GSK3β*. (A) qRT-PCR analysis of *Gsk3β* in murine iPSC^{WT} (white circles) and iPSC^{GSNOR-/-} (black circles) during cardiomyocyte differentiation. (B) S-nitrosylation of Gsk3β in murine iPSC^{GSNOR-/-} and iPSC^{WT} as assessed by SNO-RAC on Day 4. Effects on *Gsk3β* mRNA levels, in (C) murine iPSC^{WT}, following 3 h incubation with 3 different concentrations of the NO donor, GSNO, on Day 4, and in (D) hiPSCs (brown circles), following 24 h of incubation with GSNO beginning on Day 1. (E) Western blot analysis of Axin 1 and Hsp90 (internal control) in murine iPSC^{WT} (white circles) and iPSC^{GSNOR-/-} (black circles) on Day 0, 2, 4 and 6 of cardiomyocyte differentiation. qRT-PCR analysis of *Axin 1* (F) and *Axin 2* (G) in murine iPSC^{WT} (white circles) and iPSC^{GSNOR-/-} (black circles) during cardiomyocyte differentiation. Data are the mean ± SEM of 3 independent experiments. *P*-values were calculated using Student's *t*-test at each time point. **P* < 0.05.

GSNOR loss of function, affects EMT-related transcription factors in murine and human iPSCs. qRT-PCR studies revealed upregulation of *Snail 1* (Day 4), murine Snail Family Transcriptional Repressor 2 gene (*Slug*) (Day 6) and *Twist* (Days 4 and 6) mRNA and down regulation of *E-cadherin* mRNA (Day 6) in murine iPSC^{GSNOR-/-} compared to iPSC^{WT} (*P* < 0.05, [Figure 4A-D](#)). Similarly, in human iPSCs on Day 2, human Snail Family Transcriptional Repressor 1 gene (*SNAIL*) and human Snail Family Transcriptional Repressor 2 gene (*SLUG*) were upregulated following 24 h treatment with 250 μM GSNO [[Figure 4E and F](#)], although the *GSK3β* expression was reduced with 100 μM GSNO. These data suggest that the decreased *Gsk3β* expression/activity observed in iPSC^{GSNOR-/-} is associated with the early initiation of EMT and resulting in enhanced cell proliferation.

GSNOR deletion reduces Brachyury (T) and promotes early cardiac differentiation

Multiple upstream signals regulate the mesoderm marker, brachyury expression including Phosphatidylinositol-3 kinase (PI3K)/Akt pathway^[28] and GSK3β via the Wnt/β-catenin pathway^[29]. Recent work suggests that brachyury is essential for specifying cell fate but dispensable for cell survival, proliferation and EMT^[30]. Thus, we investigated the effects of altered S-nitrosylation on the function of brachyury in our iPSC model. Surprisingly, brachyury mRNA expression was reduced on Day 4 in iPSC^{GSNOR-/-} [[Figure 5A](#)]. To confirm this result, we treated iPSC^{WT} with 25 μM GSNO for 24 h on Day 4, which produced a 45% reduction in brachyury protein levels [[Figure 5B](#)]. Murine brachyury gene (*t*) mRNA levels in iPSC^{WT} treated with three different concentrations of GSNO (25 μM, 125 μM and 250 μM) for 3 h on Day 4 of differentiation were measured. A significant reduction in *t* mRNA was observed with 125 μM

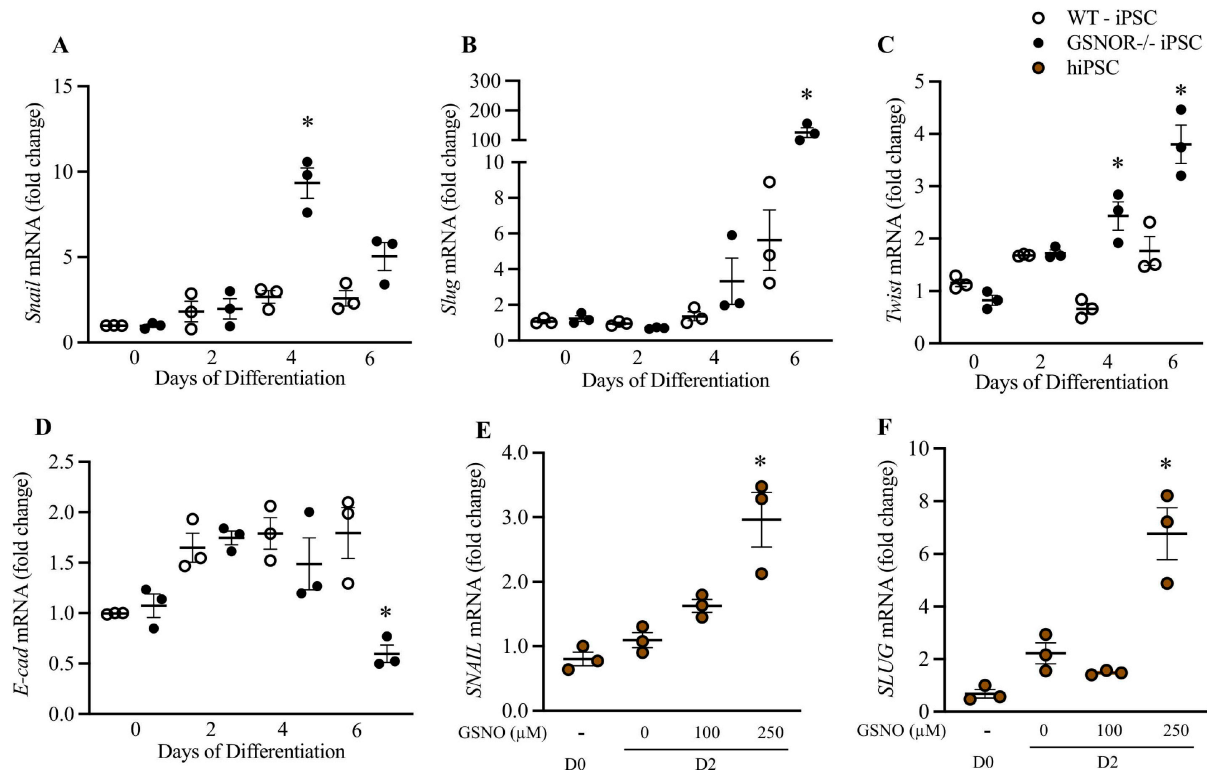


Figure 4. GSNOR loss of function regulates EMT-Related transcription factors in murine iPSC^{GSNOR^{-/-}} and hiPSCs treated with GSNO. qRT-PCR analysis of *Snail* (A), *Slug* (B), *Twist* (C) and *E-cadherin* (D) in murine iPSC^{WT} (white circles) and iPSC^{GSNOR^{-/-}} (black circles) during cardiomyocyte differentiation. qRT-PCR analysis of *SNAIL* (E) and *SLUG* (F) in hiPSC, on Day 2, following 24 h incubation with GSNO (brown circles). Data are the mean \pm SEM of 3 independent experiments. *P*-values were calculated using Student's *t*-test. **P* < 0.05.

GSNO [Figure 5C]. Using the same approach, human brachyury gene (*T*) mRNA levels in hiPSC after 24 h GSNO (on Day 2) confirmed the reduction of *T* under conditions of increased NO availability [Figure 5D]. However, there was no significant increase in *T* mRNA following treatment with 250 μ M GSNO in either miPSCs or hiPSCs, a result that can likely be explained by the biphasic effect (low and high concentration) of NO on differentiation^[23]. Our results suggest that increasing NO bioavailability reduces brachyury expression.

iPSC^{GSNOR^{-/-}} exhibited an increased percentage of beating EBs on Days 8, 10, and 11. On Day 10, 80% of iPSC^{GSNOR^{-/-}} EB outgrowth area displayed beating compared with 48% of iPSC^{WT} EBs [Figure 5E]. Representative images of organoids [Figure 5F] and video of beating organoids was captured by standard brightfield microscopy (Supplementary Movie 1 - beating organoids of iPSC^{WT}; Supplementary Movie 2 - beating organoids of iPSC^{GSNOR^{-/-}}). In addition to brachyury, mRNA for stage-specific markers of cardiac mesoderm (*Isl1*) and cardiac progenitors (*Nkx 2.5* and *Gata4*) were also altered at specific timepoints in iPSC^{GSNOR^{-/-}} compared to iPSC^{WT}. *Isl1* expression was decreased and *Nkx 2.5* was significantly increased on Day 4 while *Gata4* expression was decreased on Day 6 [Figure 5G]. *Mesp1* expression was not different between the two iPSCs [Figure 5G]. Together, these results demonstrate that increased NO bioavailability in iPSC^{GSNOR^{-/-}} promotes a faster transition from mesoderm to cardiac progenitor, as measured by increasing *Nkx 2.5* expression.

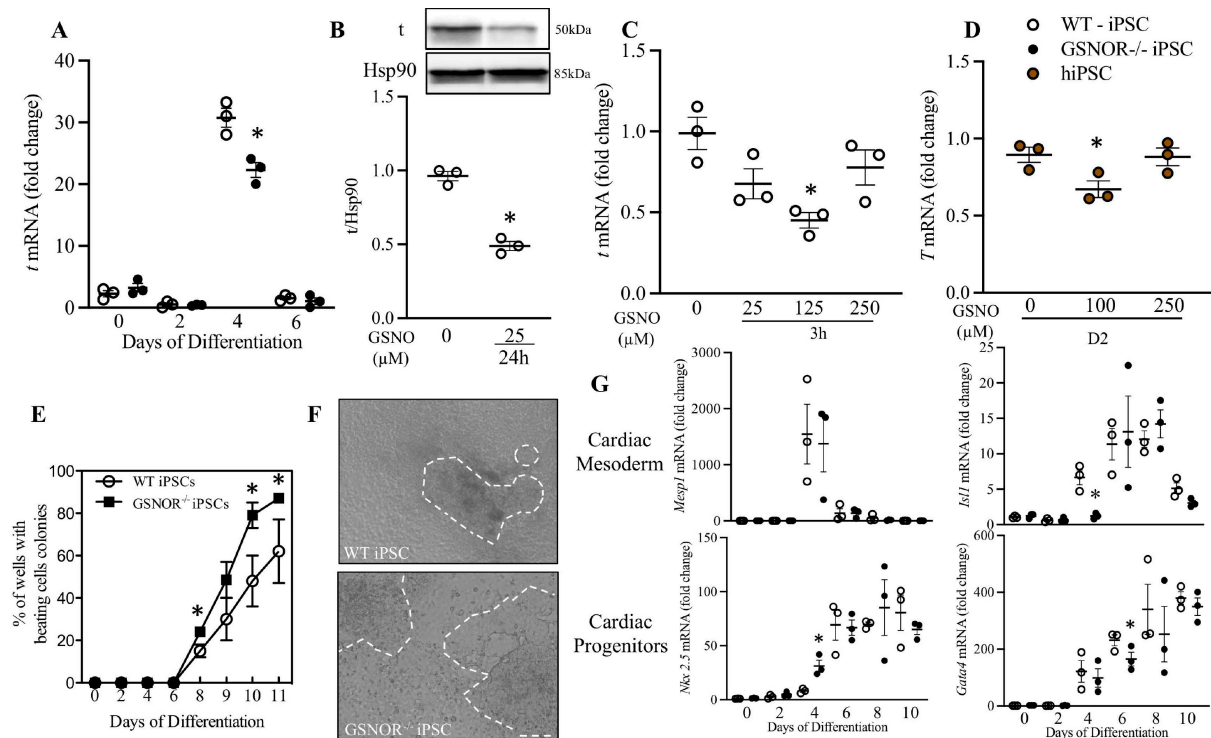


Figure 5. GSNOR loss of function reduces Brachyury (*T*) and accelerates cardiomyocyte differentiation. (A) qRT-PCR analysis of *t* in murine iPSC^{WT} (white circles) and iPSC^{GSNOR^{-/-}} (black circles) during cardiomyocyte differentiation. WB (B) and qRT-PCR (C) of *t* in murine iPSC^{WT} on Day 4, following 24 h of incubation with GSNO. (D) qRT-PCR analysis of *T* in hiPSC, on Day 2, following 24 h incubation with GSNO. (E) Percentage of beating colonies from murine iPSC^{WT} and iPSC^{GSNOR^{-/-}} during cardiomyocyte differentiation. (F) Representative images of organoids from murine iPSC^{WT} (top) iPSC^{GSNOR^{-/-}} (bottom) on Day 10 of cardiomyocyte differentiation. (G) qRT-PCR analysis of Cardiac mesoderm (*Mesp1*, *Isl1*) and Cardiac Progenitors genes (*Nkx 2.5*, *Gata4*) in murine iPSC^{WT} and iPSC^{GSNOR^{-/-}} during cardiomyocyte differentiation. Data are the mean ± SEM of 3 independent experiments. *P*-values were calculated using Student's *t*-test. **P* < 0.05.

GSNOR deletion impacts cardiomyocyte structural maturation

As CM differentiation progresses, there are specific isoform switches of structural proteins indicative of the maturity of differentiating CMs, e.g., increased myosin heavy chain MYH6/MYH7 and troponin I ssTNI/TNNi1 to cTNI/TNNi3 expression ratios, and the emergence of genes involved in calcium handling, such as *RyR2*, sarco(endo)plasmic reticulum Ca²⁺-ATPase (*SERCA*) and Na⁺/Ca²⁺ exchanger (*NCX*)^[31]. To understand the maturation of our undifferentiated iPSCs into cardiomyocytes, and to assess the impact of S-nitrosylation on this process, we investigated the expression of these CM-related genes on Days 10 and 21 of differentiation/maturation. *Tnni1* expression was increased on Day 10 in iPSC^{GSNOR^{-/-}} compared to iPSC^{WT}. *Tnni3* was detected at the early stage (Day 0), followed by a sharp decrease and a gradual increase thereafter. For this gene, we observed a significant increase in iPSC^{GSNOR^{-/-}} on Day 4 and Day 10 [Figure 6A]. Immunofluorescence analyses confirmed our previous results that troponin I expression increased on Day 10 in the iPSC^{GSNOR^{-/-}} [Figure 6B]. Following typical differentiation protocols, the sarcomeres of hPSC-CMs are usually composed of a mixture of α (MYH6) and β (MYH7) isoforms of the myosin heavy chain^[32]. In our study, both *Myh6* or *Myh7* expression were significantly increased in iPSC^{GSNOR^{-/-}}-CMs compared to iPSC^{WT} on Days 8 and 10 [Figure 6A]. We evaluated the expression of markers of cardiomyocyte maturation, including structural proteins, with increasing differentiation time (Day 21). *Tnni1*, *Tnni3*, *Myh6*, and *Myh7* were significantly increased in iPSC^{GSNOR^{-/-}}-CMs compared to iPSC^{WT}-CMs on Day 21 [Figure 6C]. We next evaluated the presence and relative expression of the mature calcium-handling molecular components, *RyR2* and *Atp2a2*, in miPSC-CMs. Both genes were expressed at significantly higher

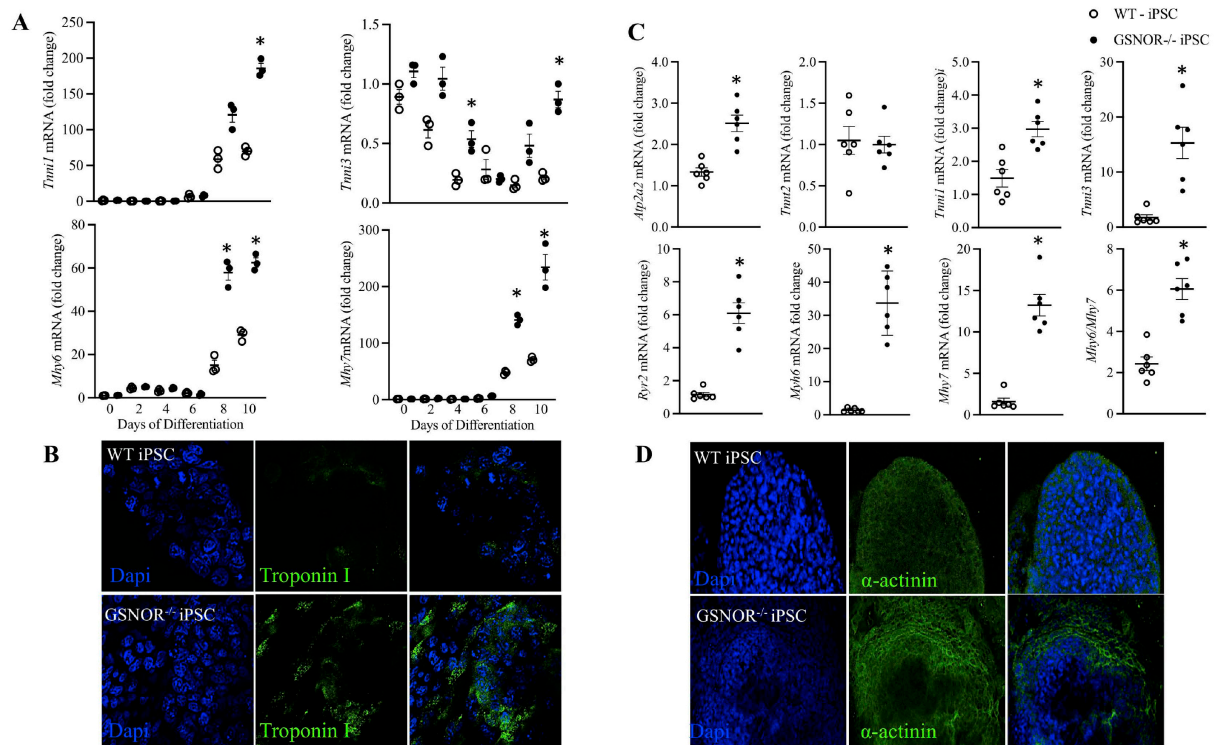


Figure 6. GSNOR loss of function impacts cardiomyocyte structural maturation. (A) qRT-PCR analysis of Cardiac genes, troponin I1 and I3 (*Tnni1*, *Tnni3*), myosin heavy chain isoforms-6 (*Myh6*) and -7 (*Myh7*) in murine iPSC^{WT} (white circles) and iPSC^{GSNOR^{-/-}} (black circles) during cardiomyocyte differentiation. (B) Representative immunofluorescence staining of Troponin I in outgrowth of beating EBs on Day 10 of murine iPSC^{WT} (top) iPSC^{GSNOR^{-/-}} (bottom). (C) qRT-PCR analysis of Myocardial genes associated with calcium (Ca²⁺) handling and cardiac contraction/relaxation, including sarco/endoplasmic reticulum Ca²⁺ ATPase 2 [sarco(endo)plasmic reticulum Ca²⁺-ATPase, murine gene (*Serca2*), troponin T2 (*Tnnt2*), *Tnni1*, *Tnni3*, type 2 ryanodine receptor (*RyR2*), *Myh6*, *Myh7*, and the *Myh6/Myh7* ratio in murine iPSC^{WT} and iPSC^{GSNOR^{-/-}}. (D) Representative immunofluorescence staining of α -actinin in outgrowths of beating iPSC^{WT} and iPSC^{GSNOR^{-/-}} EBs on Day 10. Data are the mean \pm SEM of 3 independent experiments. *P*-values were calculated using Student's *t*-test. **P* < 0.05.

levels in iPSC^{GSNOR^{-/-}} compared to iPSC^{WT}. We also observed that the sarcomere appeared better organized in iPSC^{GSNOR^{-/-}} on Day 21 as revealed by α -actinin staining [Figure 6D]. These results of structural proteins, calcium handling genes, and sarcomeric α -actinin suggest that, at this stage of cardiomyocyte differentiation of iPSC^{GSNOR^{-/-}} is more advanced than iPSC^{WT}.

The absence of GSNOR impacts Calcium handling

Ca²⁺ signaling within early cardiac progenitors may be important to promote sufficient differentiation for subsequent contractile function^[33,34]. To obtain mechanistic insight into the onset of Ca²⁺ handling in our model and its impact on CM differentiation, recording of calcium transients with fluorescent indicators was performed. We compared Ca²⁺ handling in iPSC^{WT}- and iPSC^{GSNOR^{-/-}}-derived CMs on Day 10 and 21 of differentiation. Both strains exhibited properly shaped Ca²⁺ transients (spontaneous or electrically induced), Figure 7A and B, and a functional SR, since Ca²⁺ was released by activating the ryanodine receptor (RyR2) with 20 mM caffeine [Figure 7A]. However, iPSC^{GSNOR^{-/-}}-CMs from Day 10 responded to 4 Hz pacing, whereas iPSC^{WT}-CMs did not, although both strains responded to 4 Hz stimulation at Day 21 [Figure 7C]. Hence, we investigated the time dependence of changes in intracellular Ca²⁺ cycling in more detail. The Ca²⁺ transient peaks were higher in iPSC^{GSNOR^{-/-}} CMs (Figure 7C, *P* < 0.0001 on Day 10 and *P* < 0.0001 on Day 21) and the time to reach those Ca²⁺ transient peaks was shorter compared with iPSC^{WT} CMs (Figure 7D, *P* < 0.0001 on Day 10 and *P* < 0.0016 on Day 21), suggesting a more efficient Ca²⁺-induced Ca²⁺ release (CICR)

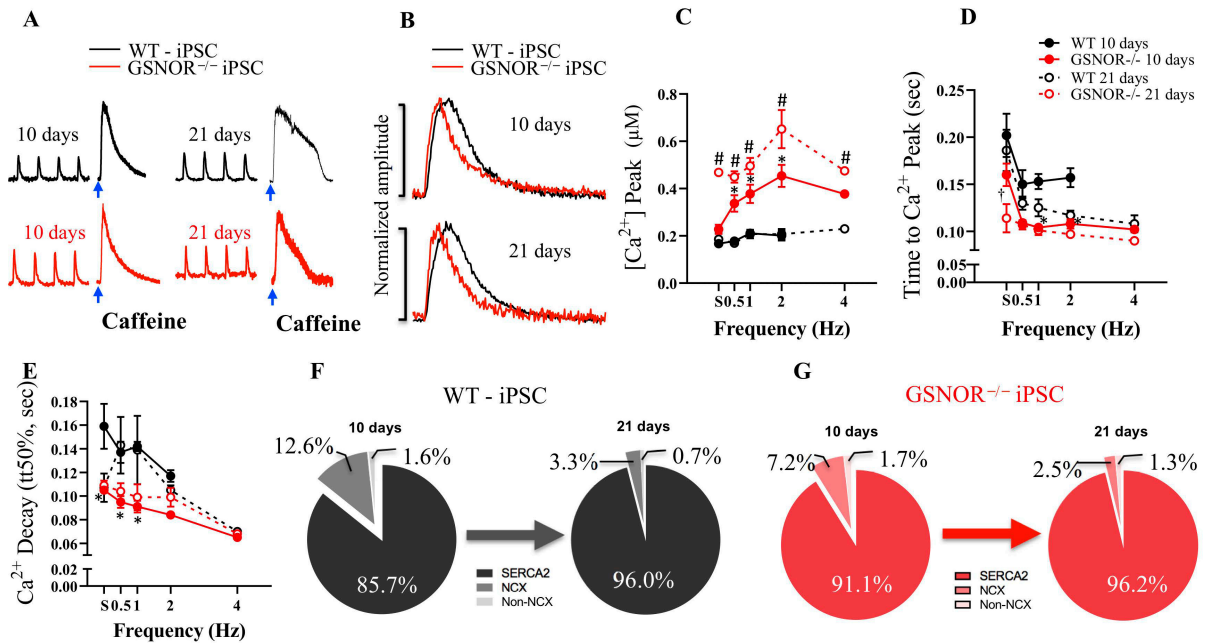


Figure 7. GSNOR loss of function promotes electrophysiological maturation of miPSC-derived CMs. (A) Representative Ca^{2+} transients in iPSC^{WT} (top, black) and $\text{iPSC}^{\text{GSNOR}^{-/-}}$ (bottom, red) mice, under electric-field stimulation at 1 Hz and under caffeine-induced (τ_{Caff} , τ_{Caff} 0Na) at Day 10, and 21 during iPSC-CM differentiation. (B) Superimposed normalized Ca^{2+} transient amplitude from iPSC^{WT} and $\text{iPSC}^{\text{GSNOR}^{-/-}}$ mice at Day 10, and 21 after iPSC-CM differentiation. (C) Average Ca^{2+} peak in response to the increasing frequency of stimulation in iPSC^{WT} (black) and $\text{iPSC}^{\text{GSNOR}^{-/-}}$ (red) mice at Day 10 and 21 after iPSC-CM differentiation. (D) Average time to Ca^{2+} peak in response to the increasing frequency of stimulation in iPSC^{WT} and $\text{iPSC}^{\text{GSNOR}^{-/-}}$ mice at Day 10 and 21 after iPSC-CM differentiation. (E) Average time to half Ca^{2+} decay ($\text{tt}50\%$) (from exponential fit) of iPSC^{WT} (black) and $\text{iPSC}^{\text{GSNOR}^{-/-}}$ (red) at Day 10 and 21 after iPSC-CM differentiation. (F) Relative contribution of the three Ca^{2+} transport systems (SERCA, NCX, non-NCX) in iPSC^{WT} and (G) $\text{iPSC}^{\text{GSNOR}^{-/-}}$ mice at Day 10 and 21 after iPSC-CM differentiation. Data are the mean \pm SEM of 3 independent experiments. *P*-values were calculated using two-way ANOVA. (**P* < 0.0001 on Day 10; #*P* < 0.0001 on Day 21; †*P* < 0.0016 on Day 21).

mechanism in cells lacking GSNOR. Likewise, the Ca^{2+} transient decay rate (shown as $\text{tt}50\%$, Figure 7E) was, overall, significantly lower in $\text{iPSC}^{\text{GSNOR}^{-/-}}$ -CMs (Figure 7E, *P* < 0.0001 on Day 10). Next, we calculated the relative contribution of the three main mechanisms involved in the cytosolic Ca^{2+} uptake and removal (SERCA, NCX, Non-NCX) in our miPSC lines at Day 10 and 21 of differentiation [Figure 7F and G]. The main mechanism involved in Ca^{2+} decay in fully mature cells is re-uptake into the SR. Cytosolic Ca^{2+} re-uptake into the SR occurs through SERCA. NCX plays a major role in Ca^{2+} handling in early, developing CMs; however, it plays a more modest role in removing Ca^{2+} from the CM in mature cells. Consistently, SERCA activity (involved in SR Ca^{2+} re-uptake) was more prominent than the participation of $\text{Na}^+/\text{Ca}^{2+}$ exchanger (NCX) or other non-NCX mechanisms (both involved in removing Ca^{2+} from the cell) in both types of iPSCs. The contribution of SERCA at Day 10 was significantly higher in $\text{iPSC}^{\text{GSNOR}^{-/-}}$ compared to iPSC^{WT} (91.1% vs. 85.7%, respectively), depicting an advanced SR maturation in $\text{iPSC}^{\text{GSNOR}^{-/-}}$, whereas at Day 21 both iPSCs exhibited approximately 96% contribution by SERCA. Additionally, the contribution of NCX and Non-NCX was smaller in $\text{iPSC}^{\text{GSNOR}^{-/-}}$ compared to iPSC^{WT} on Day 10 and 21. Therefore, Ca^{2+} re-uptake into the SR was favored due to greater participation of SERCA over NCX in both groups, indicating an advanced state of SR maturation. However, intracellular Ca^{2+} was more efficiently handled in $\text{iPSC}^{\text{GSNOR}^{-/-}}$ either as spontaneous Ca^{2+} transients or in response to electric field-stimulation. Overall, these data indicate that at Day 10 and 21 of differentiation, the $\text{iPSC}^{\text{GSNOR}^{-/-}}$ -CMs are more mature than iPSC^{WT} -CMs.

DISCUSSION

Our report is the first to show that GSNOR loss of function and S-nitrosylation more generally, accelerate the early stage of cardiomyogenesis as modeled by iPSCs. iPSC^{GSNOR^{-/-}} exhibited earlier onset EMT and increased cellular migration and proliferation. Moreover, the maturity of differentiating cardiomyocytes, as represented by the expression of structural proteins, Ca²⁺ transients and emergent genes involved in calcium handling, and sarcomere organization, revealed by α -actinin expression, occurred earlier in iPSC^{GSNOR^{-/-}}. GSNOR loss of function increased S-nitrosylation and decreased expression and function of GSK3 β , with a concomitant increase of EMT-related transcription factors (*Snail*, *Slug* and *Twist*) but decreased *E-cadherin* [Figure 8], results that were also seen in iPSC^{WT} and hiPSC following exposure to an NO donor. *Nkx 2.5* was significantly increased upon directed differentiation toward cardiomyocytes, while brachyury, *Isl1*, and *Gata4* mRNA were decreased in iPSC^{GSNOR^{-/-}} on Day 4. Therefore, GSNOR loss of function promoted the transition from mesoderm to cardiac progenitor and accelerated cardiomyocyte differentiation at the transcription level, as early as the start of adherent culture.

Stem cell pluripotency and differentiation are regulated by several pathways. The differentiation and maintenance of pluripotency are dependent on NO concentration. Low NO concentrations delay stem cell differentiation, inducing the expression of *Nanog*, *Oct4*, and *Sox2*, and the activation of survival pathways^[23], whereas high NO concentrations, as seen in iPSC^{GSNOR^{-/-}}, induce differentiation^[35]. Consistent with this concept, we found that iPSC^{GSNOR^{-/-}} down-regulated *Oct4* and *Sox2*; however, *Klf4* was increased.

The major regulatory pathway of protein S-NO is via the metabolism of GSNO by GSNOR^[36]. GSNO exists in a steady state with protein S-NO and cardiomyocytes use GSNO as a physiologic reservoir for NO, a major participant in *trans*-S-nitrosation reactions^[37]. We showed that *Gsnor* mRNA and protein were present at Day 0 in iPSC^{WT} but, as expected, not in iPSC^{GSNOR^{-/-}}, suggesting that the changes we observed are directly associated with the absence of GSNOR function.

At the start of adherent culture, on Day 4, cell proliferation/differentiation and the activation of EMT were seen only in iPSC^{GSNOR^{-/-}}. EMT is dependent on and orchestrated by Wnt/ β -catenin signaling, consistent with its role during vertebrate heart development^[38]. Wnt/ β -catenin signaling may regulate the self-renewal of hPSCs^[39]. Inactivation of GSK3 β , a central regulator of the Wnt/ β -catenin pathway, enables the accumulation of β -catenin, initially in the cytosol, and subsequently in the nucleus, where β -catenin forms a complex with transcription factor (TCF) proteins to activate Wnt pathway gene targets^[40,41]. Wnt/ β -catenin target genes regulate the expression of pluripotency and developmental factors associated with the primitive streak and early-stage germ layers^[42]. Short-term Wnt induction maintains pluripotency, whereas long-term induction, in response to GSK3 β inhibition, induces stem cell differentiation into endo- and mesoderm derivatives^[43]. Increased S-nitrosylation of Gsk3 β in iPSC^{GSNOR^{-/-}} and hiPSCs treated with GSNO likely maintains long-term Wnt induction, promoting expression of the EMT transcriptional activators, *Snail*, *Slug*, and *Twist* and reducing *E-cadherin*. However, the relationship between elevated NO and EMT is complicated. NO at subtoxic concentrations inhibits EMT and metastasis in metastatic cell lines by upregulating RKIP and E-cadherin protein^[44]. These opposite effects may be related to an NO “threshold” that is dependent on cell type.

The regulation of Gsk3 β activity is a complex process that can be mediated by multiple mechanisms including phosphorylation/dephosphorylation, S-nitrosylation, subcellular localization, protein-protein interactions, and proteolytic cleavage^[45]. Subcellular localization of GSK3 β can also modulate its enzymatic activity^[15]. Moreover, S-nitrosylation of GSK3 β inhibits its activity^[15]. CM-specific deletion of GSK3 family members induces CM proliferation^[46,47], and the degree of this proliferation is amplified in the setting of

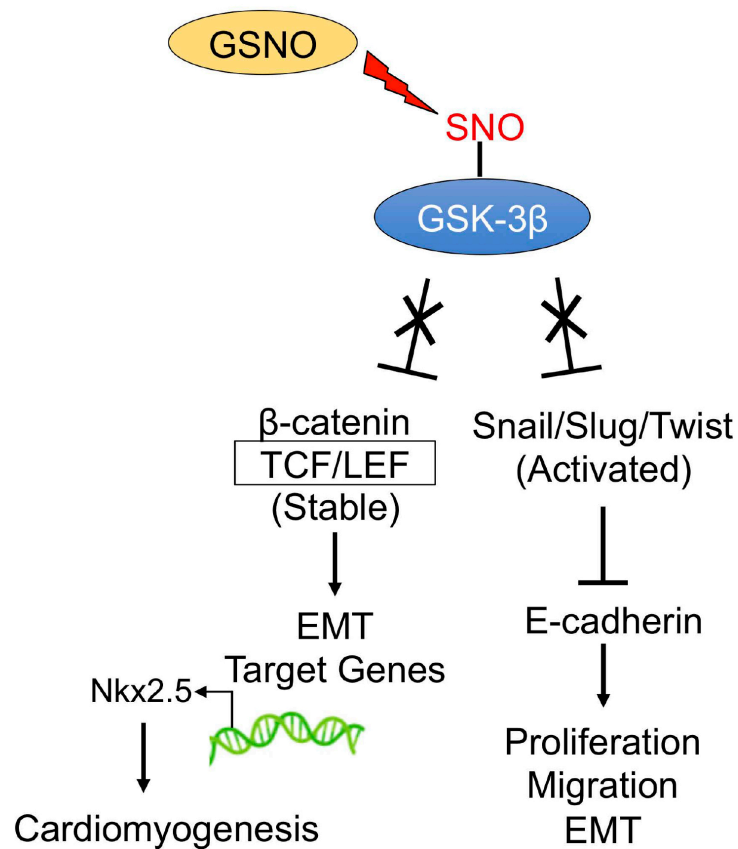


Figure 8. Schematic diagram of the proposed signaling mechanism that stimulates EMT and cardiomyogenesis. GSNOR loss of function results in GSNO accumulation and increased S-nitrosylation and reduced activity of GSK-3 β , a protein that targets *Snail/Slug/Twist* and β -catenin for degradation through the ubiquitin proteasome pathway. This increased β -catenin and *Snail/Slug/Twist* represses E-cadherin, promotes β -catenin association with TCF/LEF complexes, augmenting transcription of proliferation, migration, EMT, and other target genes, resulting in elevated levels of *Nkx2.5* mRNA levels and accelerating cardiomyogenesis.

cardiac stress^[48]. Our results also demonstrated that a reduction of GSK3 β by S-nitrosylation resulted in increased proliferation but coupled with differentiation. However, the precise molecular mechanism for this shift from proliferating to terminally differentiated CMs is unclear, and currently of great scientific interest. Elucidating these mechanisms will provide novel strategies to reverse this terminally differentiated state, allowing CMs to resume proliferation.

Axins were significantly increased on Day 4, in iPSC^{GSNOR^{-/-}} cells. Both Axin and its homolog Axin2 act as scaffold proteins, which bind several components of the canonical Wnt signaling pathway^[49]. Axin2, a bona fide downstream target of canonical Wnt, participates in a negative feedback loop, which could serve to limit the duration or intensity of a Wnt-initiated signal^[50]. Moreover, Axin2 increases canonical TCF/LEF activity and Snail-mediated EMT progression^[51]. Here, we observed increased levels of *Axin2*, which might indicate activation of the canonical Wnt pathway, likely secondary to the inactivation of GSK3 β upon its S-nitrosylation. There may be at least two pools of GSK3 β in cells, one associated with Axin and refractory to phosphorylation by Akt, and another that can be regulated by Akt^[52]. Our findings complement a positive regulatory function for Axin1 and Axin2 in Wnt signaling^[53] in developing CMs.

The differentiation of stem cells along the cardiac lineage is characterized by the early expression of a network of mesodermal-cardiac transcription factors, that activate gene expression for structural proteins such as MHC, *Mlc2v*, α -actinin, and troponin. Upon directed differentiation toward cardiomyocytes, pluripotent cells first pass through a progenitor stage, identified by the expression of specific transcription factors, such as brachyury in the mesoderm stage (early phase) and *Nkx 2.5*, *Gata4*, *Mef2c* in the cardiac progenitor cell stage (later phase)^[54]. We showed that iPSCs^{GSNOR^{-/-}} expression of markers of mesoderm induction (*t*-brachyury); cardiac mesoderm (*Isl1*); and cardiac progenitors (*Gata4*) were reduced, whereas, *Nkx 2.5*, a cardiac progenitor marker, was increased. In murine embryonic stem cells, exposure to the NO donor, diethylenetriamine/nitric oxide adduct can repress *brachyury*, *Gata4*, *Gata6*, Fibroblast growth factor (Fgf) 5, and *Fgf8*^[23]. Following cardiogenic differentiation, *Isl1* is progressively repressed, and only a small number of *Isl1*⁺ cells remain in the postnatal heart^[55].

Similar to other post-translational modifications (i.e., phosphorylation, methylation, acetylation), S-NO regulates the expression and function of key proteins controlling mammalian cell differentiation^[5] and cell-cycle activity^[56]. In the adult heart, S-NO modulates signaling pathways important for vasodilation, cardiomyocyte contraction, mitochondrial function^[57], and Ca^{2+} handling^[3,58]. In murine embryonic stem cells^[2], an isotope labeling proteomics screening approach, demonstrated that Prdx-2 nitrosylation (following GSNO exposure) favors cardiomyocyte differentiation. Although an increased percentage of beating cells was observed in iPSCs^{GSNOR^{-/-}} on Day 8, significant changes occur as the cells continue to develop. Therefore, we followed the progress of cell differentiation until Day 21. In addition, NO improves calcium handling in mature cardiomyocytes^[59]; however, the acute and chronic effects on differentiating cardiomyocytes have not been elucidated.

There is no current understanding regarding the onset of Ca^{2+} handling and its impact on differentiation and cardiogenesis. However, Ca^{2+} transients, calcium handling-related gene, protein expression, and sarcomere organization were, except for *Tnnt2*, all significantly increased on Days 10 and 21 in iPSC^{GSNOR^{-/-}} compared to iPSC^{WT}. These results are supported by the observation that the NO-donor, CysNO, upregulated β MHC, producing a higher β MHC to α MHC ratio and superior calcium handling capabilities in EBs without altering EB size or viability^[1]. Our findings also corroborate that RyR2 S-nitrosylation increases the activity of this channel^[60]; whereas, decreased RyR2 S-nitrosylation is associated with reduced SR Ca^{2+} release^[61].

Prolonging time in culture promotes the maturation of iPSC-CMs, including more mature morphology, structure, and physiology^[62]. Our iPSC-derived CMs were grown for only 21 days. Human iPSC-derived CMs chronologically aged in vitro, exhibited accelerated senescence and functional deterioration within four months in culture, resembling cardiac tissue from a 65-year-old human^[63]. During senescence and mammalian aging, GSNOR expression declines, resulting in nitrosative stress and the accumulation of damaged mitochondria^[64]. In contrast, centenarians maintain high GSNOR expression^[64].

This study is the first to investigate the effects of GSNOR deficiency during cardiomyocyte differentiation as modeled by iPSC. However, there are limitations to this study. First, this study is limited to the early stages of differentiation of both murine and human iPSCs. Second, the heterogeneous composition of differentiating iPSCs could mask the magnitude of gene expression changes. Further evaluation, such as a directed differentiation with a monolayer culture, will allow for dissection of different stages of cardiac differentiation and a better understanding of the role of GSNOR at different stages of cardiomyocyte differentiation.

In conclusion, the absence of GSNOR accelerates cardiomyocyte maturation from iPSCs. We observed increased S-nitrosylation of GSK3 β , cellular migration, proliferation, and induction of EMT. Together, these findings have important implications and may offer insights into improving cell therapy and enhancing disease modeling in the cardiovascular system.

DECLARATIONS

Authors' contributions

Designed the study and performed experiments: Salerno AG, Wanschel ACBA, Dulce RA, Hatzistergos KE
Prepared the manuscript: Salerno AG, Wanschel ACBA, Dulce RA, Hatzistergos KE, Balkan W, Hare JM
Designed experiments, guided the interpretation of the results and edited the manuscript: Balkan W, Hare JM

Availability of data and materials

Not applicable.

Financial support and sponsorship

This work was supported by the National Institutes of Health grants R01 HL107110, R01 HL137355, R01 HL084275 and 5UM HL113460; grants from the Starr Foundation and the Soffer Family Foundation (all awarded to Hare JM); and a São Paulo Research Foundation (FAPESP) grant# 2016/01044-0 (Salerno AG) and grant# 2016/01746-4 (Wanschel ACBA).

Conflicts of interest

Hare JM reported having a patent for cardiac cell-based therapy. He holds equity in Vestion Inc. and maintains a professional relationship with Vestion Inc. as a consultant and member of the Board of Directors and Scientific Advisory Board. Hare JM is the Chief Scientific Officer, a compensated consultant and advisory board member for Longeveron, and holds equity in Longeveron. Hare JM is also the co-inventor of intellectual property licensed to Longeveron. Longeveron LLC and Vestion Inc. did not participate in funding this work. Dr. Hare's relationships are disclosed to the University of Miami, and a management plan is in place. Other authors declared that there are no conflicts of interest.

Ethical approval and consent to participate

The Institutional Animal Care and Use Committee (IACUC) approved the animal studies described in this paper as Protocol #20-168.

Consent for publication

Not applicable.

Copyright

© The Author(s) 2021.

REFERENCES

1. Hodge AJ, Zhong J, Lipke EA. Enhanced stem cell-derived cardiomyocyte differentiation in suspension culture by delivery of nitric oxide using S-nitrosocysteine. *Biotechnol Bioeng* 2016;113:882-94. [DOI](#) [PubMed](#)
2. Wu B, Yu H, Wang Y, et al. Peroxiredoxin-2 nitrosylation facilitates cardiomyogenesis of mouse embryonic stem cells via XBP-1s/PI3K pathway. *Free Radic Biol Med* 2016;97:179-91. [DOI](#) [PubMed](#)
3. Dulce RA, Mayo V, Rangel EB, Balkan W, Hare JM. Interaction between neuronal nitric oxide synthase signaling and temperature influences sarcoplasmic reticulum calcium leak: role of nitroso-redox balance. *Circ Res* 2015;116:46-55. [DOI](#) [PubMed](#) [PMC](#)
4. Haldar SM, Stamler JS. S-nitrosylation: integrator of cardiovascular performance and oxygen delivery. *J Clin Invest* 2013;123:101-10. [DOI](#) [PubMed](#) [PMC](#)
5. Cao Y, Gomes SA, Rangel EB, et al. S-nitrosoglutathione reductase-dependent PPAR γ denitrosylation participates in MSC-derived adipogenesis and osteogenesis. *J Clin Invest* 2015;125:1679-91. [DOI](#) [PubMed](#) [PMC](#)
6. Beigi F, Gonzalez DR, Minhas KM, et al. Dynamic denitrosylation via S-nitrosoglutathione reductase regulates cardiovascular function. *Proc Natl Acad Sci U S A* 2012;109:4314-9. [DOI](#) [PubMed](#) [PMC](#)

7. Chung HS, Murray CI, Venkatraman V, et al. Dual labeling biotin switch assay to reduce bias derived from different cysteine subpopulations: a method to maximize S-nitrosylation detection. *Circ Res* 2015;117:846-57. DOI PubMed PMC
8. Liu L, Yan Y, Zeng M, et al. Essential roles of S-nitrosothiols in vascular homeostasis and endotoxic shock. *Cell* 2004;116:617-28. DOI PubMed
9. Hatzistergos KE, Paulino EC, Dulce RA, et al. S-nitrosoglutathione reductase deficiency enhances the proliferative expansion of adult heart progenitors and myocytes post myocardial infarction. *J Am Heart Assoc* 2015;4:e001974. DOI PubMed PMC
10. Ohta S, Suzuki K, Tachibana K, Tanaka H, Yamada G. Cessation of gastrulation is mediated by suppression of epithelial-mesenchymal transition at the ventral ectodermal ridge. *Development* 2007;134:4315-24. DOI PubMed
11. Thiery JP, Sleeman JP. Complex networks orchestrate epithelial-mesenchymal transitions. *Nat Rev Mol Cell Biol* 2006;7:131-42. DOI PubMed
12. Zhou BP, Deng J, Xia W, et al. Dual regulation of snail by GSK-3 β -mediated phosphorylation in control of epithelial-mesenchymal transition. *Nat Cell Biol* 2004;6:931-40. DOI PubMed
13. Burridge PW, Matsa E, Shukla P, et al. Chemically defined generation of human cardiomyocytes. *Nat Methods* 2014;11:855-60. DOI PubMed PMC
14. Kattman SJ, Witty AD, Gagliardi M, et al. Stage-specific optimization of activin/nodal and BMP signaling promotes cardiac differentiation of mouse and human pluripotent stem cell lines. *Cell Stem Cell* 2011;8:228-40. DOI PubMed
15. Wang SB, Venkatraman V, Crowgey EL, et al. Protein S-nitrosylation controls glycogen synthase Kinase 3 β function independent of its phosphorylation state. *Circ Res* 2018;122:1517-31. DOI PubMed PMC
16. Uosaki H, Magadam A, Seo K, et al. Identification of chemicals inducing cardiomyocyte proliferation in developmental stage-specific manner with pluripotent stem cells. *Circ Cardiovasc Genet* 2013;6:624-33. DOI PubMed PMC
17. Guide for the care and use of laboratory animals. 8th ed, National Academies Press, 2010. DOI
18. Lian X, Hsiao C, Wilson G, et al. Robust cardiomyocyte differentiation from human pluripotent stem cells via temporal modulation of canonical Wnt signaling. *Proc Natl Acad Sci U S A* 2012;109:E1848-57. DOI PubMed PMC
19. Forrester MT, Thompson JW, Foster MW, Nogueira L, Moseley MA, Stampler JS. Proteomic analysis of S-nitrosylation and denitrosylation by resin-assisted capture. *Nat Biotechnol* 2009;27:557-9. DOI PubMed PMC
20. Bloch W, Fleischmann BK, Lorke DE, et al. Nitric oxide synthase expression and role during cardiomyogenesis. *Cardiovasc Res* 1999;3:675-84. DOI PubMed
21. Takahashi K, Tanabe K, Ohnuki M, et al. Induction of pluripotent stem cells from adult human fibroblasts by defined factors. *Cell* 2007;131:861-72. DOI PubMed
22. Li HX, Han M, Bernier M, et al. Krüppel-like factor 4 promotes differentiation by transforming growth factor- β receptor-mediated Smad and p38 MAPK signaling in vascular smooth muscle cells. *J Biol Chem* 2010;285:17846-56. DOI PubMed PMC
23. Tejedo JR, Tapia-Limonchi R, Mora-Castilla S, et al. Low concentrations of nitric oxide delay the differentiation of embryonic stem cells and promote their survival. *Cell Death Dis* 2010;1:e80. DOI PubMed PMC
24. Saraiva RM, Minhas KM, Raju SV, et al. Deficiency of neuronal nitric oxide synthase increases mortality and cardiac remodeling after myocardial infarction: role of nitroso-redox equilibrium. *Circulation* 2005;112:3415-22. DOI PubMed
25. Fu K, Chronis C, Soufi A, et al. Comparison of reprogramming factor targets reveals both species-specific and conserved mechanisms in early iPSC reprogramming. *BMC Genomics* 2018;19:956. DOI PubMed PMC
26. Bachelder RE, Yoon SO, Franci C, de Herrerros AG, Mercurio AM. Glycogen synthase kinase-3 is an endogenous inhibitor of Snail transcription: implications for the epithelial-mesenchymal transition. *J Cell Biol* 2005;168:29-33. DOI PubMed PMC
27. Wang Y, Liu J, Ying X, Lin PC, Zhou BP. Twist-mediated epithelial-mesenchymal transition promotes breast tumor cell invasion via inhibition of hippo pathway. *Sci Rep* 2016;6:24606. DOI PubMed PMC
28. Otani R, Mukasa A, Shin M, et al. Brachyury gene copy number gain and activation of the PI3K/Akt pathway: association with upregulation of oncogenic Brachyury expression in skull base chordoma. *J Neurosurg* 2018;128:1428-37. DOI PubMed
29. Yan X, Li Z, Li H, et al. Inhibition of glycogen synthase kinase 3 β suppresses the growth and survival of skull base chordoma cells by downregulating brachyury expression. *Oncotargets Ther* 2019;12:9783-91. DOI PubMed PMC
30. Zhu J, Kwan KM, Mackem S. Putative oncogene brachyury (T) is essential to specify cell fate but dispensable for notochord progenitor proliferation and EMT. *Proc Natl Acad Sci U S A* 2016;113:3820-5. DOI PubMed PMC
31. Bedada FB, Chan SS, Metzger SK, et al. Acquisition of a quantitative, stoichiometrically conserved ratiometric marker of maturation status in stem cell-derived cardiac myocytes. *Stem Cell Reports* 2014;3:594-605. DOI PubMed PMC
32. Weber N, Schwanke K, Greten S, et al. Stiff matrix induces switch to pure β -cardiac myosin heavy chain expression in human ESC-derived cardiomyocytes. *Basic Res Cardiol* 2016;111:68. DOI PubMed
33. Mesaeli N, Nakamura K, Zvaritch E, et al. Calreticulin is essential for cardiac development. *J Cell Biol* 1999;144:857-68. DOI PubMed PMC
34. Li J, Pucéat M, Perez-Terzic C, et al. Calreticulin reveals a critical Ca(2+) checkpoint in cardiac myofibrillogenesis. *J Cell Biol* 2002;158:103-13. DOI PubMed PMC
35. Mora-Castilla S, Tejedo JR, Hmadcha A, et al. Nitric oxide repression of Nanog promotes mouse embryonic stem cell differentiation. *Cell Death Differ* 2010;17:1025-33. DOI PubMed
36. Benhar M, Forrester MT, Stampler JS. Protein denitrosylation: enzymatic mechanisms and cellular functions. *Nat Rev Mol Cell Biol* 2009;10:721-32. DOI PubMed
37. Kohr MJ, Aponte AM, Sun J, et al. Characterization of potential S-nitrosylation sites in the myocardium. *Am J Physiol Heart Circ Physiol* 2011;300:H1327-35. DOI PubMed PMC

38. Lickert H, Kutsch S, Kanzler B, Tamai Y, Taketo MM, Kemler R. Formation of multiple hearts in mice following deletion of β -catenin in the embryonic endoderm. *Dev Cell* 2002;3:171-81. DOI PubMed
39. Sato N, Meijer L, Skaltsounis L, Greengard P, Brivanlou AH. Maintenance of pluripotency in human and mouse embryonic stem cells through activation of Wnt signaling by a pharmacological GSK-3-specific inhibitor. *Nat Med* 2004;10:55-63. DOI PubMed
40. McCubrey JA, Steelman LS, Bertrand FE, et al. GSK-3 as potential target for therapeutic intervention in cancer. *Oncotarget* 2014;5:2881-911. DOI PubMed PMC
41. Nakamura M, Liu T, Husain S, et al. Glycogen Synthase kinase-3 α promotes fatty acid uptake and lipotoxic cardiomyopathy. *Cell Metab* 2019;29:1119-1134.e12. DOI PubMed PMC
42. Hödar C, Assar R, Colombres M, et al. Genome-wide identification of new Wnt/ β -catenin target genes in the human genome using CART method. *BMC Genomics* 2010;11:348. DOI PubMed PMC
43. Huang TS, Li L, Moalim-Nour L, et al. A regulatory network involving β -catenin, e-cadherin, PI3k/Akt, and slug balances self-renewal and differentiation of human pluripotent stem cells in response to wnt signaling. *Stem Cells* 2015;33:1419-33. DOI PubMed PMC
44. Baritaki S, Huerta-Yepez S, Sahakyan A, et al. Mechanisms of nitric oxide-mediated inhibition of EMT in cancer: inhibition of the metastasis-inducer Snail and induction of the metastasis-suppressor RKIP. *Cell Cycle* 2010;9:4931-40. DOI PubMed PMC
45. Mirzoev TM, Sharlo KA, Shenkman BS. The role of GSK-3 β in the regulation of protein turnover, myosin phenotype, and oxidative capacity in skeletal muscle under disuse conditions. *Int J Mol Sci* 2021;22:5081. DOI PubMed PMC
46. Woulfe KC, Gao E, Lal H, et al. Glycogen synthase kinase-3 β regulates post-myocardial infarction remodeling and stress-induced cardiomyocyte proliferation in vivo. *Circ Res* 2010;106:1635-45. DOI PubMed PMC
47. Matsuda T, Zhai P, Maejima Y, et al. Distinct roles of GSK-3 α and GSK-3 β phosphorylation in the heart under pressure overload. *Proc Natl Acad Sci U S A* 2008;105:20900-5. DOI PubMed PMC
48. Singh AP, Umbarkar P, Guo Y, Force T, Gupte M, Lal H. Inhibition of GSK-3 to induce cardiomyocyte proliferation: a recipe for in situ cardiac regeneration. *Cardiovasc Res* 2019;115:20-30. DOI PubMed PMC
49. Jho EH, Zhang T, Domon C, Joo CK, Freund JN, Costantini F. Wnt/ β -catenin/Tcf signaling induces the transcription of Axin2, a negative regulator of the signaling pathway. *Mol Cell Biol* 2002;22:1172-83. DOI PubMed PMC
50. Kang HE, Seo Y, Yun JS, et al. Metformin and niclosamide synergistically suppress Wnt and YAP in APC-mutated colorectal cancer. *Cancers (Basel)* 2021;13:3437. DOI PubMed PMC
51. Ahn SY, Kim NH, Lee K, et al. Niclosamide is a potential therapeutic for familial adenomatous polyposis by disrupting Axin-GSK3 interaction. *Oncotarget* 2017;8:31842-55. DOI PubMed PMC
52. Ding VW, Chen RH, McCormick F. Differential regulation of glycogen synthase kinase 3 β by insulin and Wnt signaling. *J Biol Chem* 2000;275:32475-81. DOI PubMed
53. Lui TT, Lacroix C, Ahmed SM, et al. The ubiquitin-specific protease USP34 regulates axin stability and Wnt/ β -catenin signaling. *Mol Cell Biol* 2011;31:2053-65. DOI PubMed PMC
54. Kehat I, Kenyagin-Karsenti D, Snir M, et al. Human embryonic stem cells can differentiate into myocytes with structural and functional properties of cardiomyocytes. *J Clin Invest* 2001;108:407-14. DOI PubMed PMC
55. Weinberger F, Mehrkens D, Friedrich FW, et al. Localization of Islet-1-positive cells in the healthy and infarcted adult murine heart. *Circ Res* 2012;110:1303-10. DOI PubMed PMC
56. Kunieda T, Minamino T, Miura K, et al. Reduced nitric oxide causes age-associated impairment of circadian rhythmicity. *Circ Res* 2008;102:607-14. DOI PubMed
57. Murray CI, Kane LA, Uhrigshardt H, Wang SB, Van Eyk JE. Site-mapping of in vitro S-nitrosation in cardiac mitochondria: implications for cardioprotection. *Mol Cell Proteomics* 2011;10:M110.004721. DOI PubMed PMC
58. Gonzalez DR, Treuer A, Sun QA, Stamler JS, Hare JM. S-nitrosylation of cardiac ion channels. *J Cardiovasc Pharmacol* 2009;54:188-95. DOI PubMed PMC
59. Petroff MG, Kim SH, Pepe S, et al. Endogenous nitric oxide mechanisms mediate the stretch dependence of Ca²⁺ release in cardiomyocytes. *Nat Cell Biol* 2001;3:867-73. DOI PubMed
60. Xu L, Eu JP, Meissner G, Stamler JS. Activation of the cardiac calcium release channel (ryanodine receptor) by poly-S-nitrosylation. *Science* 1998;279:234-7. DOI PubMed
61. Gonzalez DR, Beigi F, Treuer AV, Hare JM. Deficient ryanodine receptor S-nitrosylation increases sarcoplasmic reticulum calcium leak and arrhythmogenesis in cardiomyocytes. *Proc Natl Acad Sci U S A* 2007;104:20612-7. DOI PubMed PMC
62. Ahmed RE, Anzai T, Chanthra N, Uosaki H. A brief review of current maturation methods for human induced pluripotent stem cells-derived cardiomyocytes. *Front Cell Dev Biol* 2020;8:178. DOI PubMed PMC
63. Acun A, Nguyen TD, Zorlutuna P. In vitro aged, hiPSC-origin engineered heart tissue models with age-dependent functional deterioration to study myocardial infarction. *Acta Biomater* 2019;94:372-91. DOI PubMed PMC
64. Rizza S, Cardaci S, Montagna C, et al. S-nitrosylation drives cell senescence and aging in mammals by controlling mitochondrial dynamics and mitophagy. *Proc Natl Acad Sci U S A* 2018;115:E3388-97. DOI PubMed PMC